Improvement of Boron-Rich Boronitride Adhesion through Titanium Boronitride on Glass Surfaces and Optical Fibers by Diammonium Hexafluorotitanate(IV) and Borazine[⊥]

Mohamed Mokhtari,[†] Hyung S. Park,[†] Stephen E. Johnson,[‡] Wolfgang Bolse,[§] and Herbert W. Roesky*,[†]

Institut für Anorganische Chemie der Universität Göttingen, Tammannstrasse 4, D-37077 Göttingen, Germany; University of Iowa, Department of Chemistry, 473 Chemistry Botany Bldg., Iowa City, Iowa 52242-1294; and II. Physikalisches Institut der Universität Göttingen, Bunsenstrasse 7-9, D-37073 Göttingen, Germany

Received July 2, 1996. Revised Manuscript Received September 10, 1996[⊗]

Titanium boronitride (Ti−B−N) films have been produced by solid−gas reaction in the temperature range 600−700 °C using $[(NH_4)_2TiF_6]$ and $B_3N_3H_6$ (borazine) as precursors. The resulting material is deposited on SiO_2 substrates and on optical fibers, respectively. Films with thicknesses ranging from 0.3 to 1 μm possess a characteristic black color. They are stable over a wide temperature range, exhibit strong adhesion to glass and quartz glass and show resistance to mechanical deformation (i.e., fracture toughness). Furthermore, the ceramic films are not oxidized at room temperature even by strong oxidizing acids such as concentrated HNO_3. Auger electron spectroscopy (AES) depth profile analyses indicate that the Ti concentration decreases progressively from the interface to the surface of the film. Results obtained by Rutherford backscattering spectroscopy (RBS) studies agree well with those of AES. Moreover, the decomposition products of $[(NH_4)_2TiF_6]$ are involved in the reactions at the surface of the substrate, enhancing the adhesion of the film. AFM analyses show a columnar type film growth with grain sizes ranging from 200 to 700 nm. The films possess electrical resistivity and hardness on the order of 6000 $\mu\Omega$cm and 22 Gpa (Vickers), respectively.

Introduction

The synthesis of new materials with important physical and mechanical properties such as hardness (e.g., diamond),[1] chemical inertness and high thermal stability (e.g., boron nitride, BN),[2] and high electrical conductivity (e.g., titanium nitride, TiN)[3] are of great fundamental and technological interest. For example, carbides, borides, and nitrides have been increasingly used as protecting coatings for tools and machine components subject to highly complex stress conditions, which include abrasive and adhesive wear.[4] Coatings of the Ti−B−N type, in particular, have attracted interest due to their high hardness, stability at high temperatures and corrosion resistance.[5] Preparative routes to Ti−B−N coatings include chemical vapor deposition (CVD),[6] plasma-assisted CVD,[7, 8] sputtering,[9−11] and ion beam methods.[12] A recent process has been developed, involving growth of Ti−B−N coatings by subsequent annealing at moderate temperatures (400 °C), initiating an interdiffusion process that affords very hard phases.[10] We have recently developed a solid−gas reaction, motivated by the need to strictly control stoichiometry on a molecular level and for the efficient production of thin-film materials at low processing temperatures, in a reproducible manner.[13] In contrast to TiN/TiB_2 composites[14] or boron-rich boron nitride compositions (e.g., B_3N, B_5N, $B_{25}N$, $B_{53}N$),[15−18] we have prepared a stable polycrystalline compound of Ti−B−N at 700 °C. To control the processing of Ti−B−N films, an understanding of the

[⊥] Dedicated to Professor Oskar Glemser on the occasion of his 85th birthday.

[†] Universität Göttingen.

[‡] University of Iowa.

[§] Universität Göttingen.

[⊗] Abstract published in *Advance ACS Abstracts,* October 15, 1996.

(1) Spear, K. *J. Am. Ceram. Soc.* **1989**, *72*, 171.
(2) Paine, R. T.; Narula, C. K. *Chem. Rev.* **1990**, *90*, 73.
(3) Farahani, M. M.; Garg, S.; Moore, B. T. *J. Electrochem. Soc.* **1994**, *141*, 479.
(4) Gissler, W.; Friesen, T.; Haupt, J.; Rickerby, D. G. *Spec. Publ., R. Soc. Chem.* **1993**, *126*, 320.
(5) Matthes, B.; Broszeit, E.; Kloos, K. H. *Surf. Coat. Technol.* **1993**, *57*, 97.
(6) Peytavy, J. L.; Lebugle, A.; Montel, G.; Pastor, H. *High Temp.-High Press.* **1978**, *10*, 341.
(7) Aromaa, J.; Ronkainen, H.; Mahiout, A.; Hannula, S. P.; Leyland, A.; Matthews, A.; Matthes, B.; Broszeit, E. *Mater. Sci. Eng.* **1991**, *A140*, 722.
(8) Karner, H.; Laimer, J.; Störi, H.; Rödhammer, P. *Surf. Coat. Technol.* **1989**, *39/40*, 293.
(9) Herr, W.; Matthes, B.; Broszeit, E.; Kloos, K. H. *Mater. Sci. Eng.* **1991**, *A140*, 616.
(10) Frisien, T.; Haupt, J.; Gissler, W.; Barna, A.; Barna, P. B. *Surf. Coat. Technol.* **1991**, *48*, 1.
(11) Mitterer, C.; Rauter, M.; Rödhammer, P. *Surf. Coat. Technol.* **1990**, *41*, 351.
(12) Yang, Q. Q.; Wen, L. S.; Chen, X. Z.; Zheng, Y. Q.; Zhuang, Y. Z. *Vacuum* **1995**, *46*, 181.
(13) Mokhtari, M.; Park, H. S.; Roesky, H. W.; Johnson, S. E.; Bolse, W.; Conrad, J.; Plass, W. *Chem. A Eur. J.* **1996**, *2*, 1269.
(14) Nowakowski, M.; Su, K.; Sneddon, L.; Bonnel, D. *Mater. Res. Soc. Symp. Proc.* **1993**, *286*, 425.
(15) Will, G.; Kossobutzki, K. H. *J. Less-Common Met.* **1976**, *47*, 33.
(16) Ploog, K.; Rauh, P.; Stoeger, W.; Schmidt, H. *J. Cryst. Growth* **1972**, *13/14*, 350.
(17) Saitoh, H.; Yoshida, K.; Yarborough, W. A. *J. Mater. Res.* **1993**, *8*, 8.
(18) Ploog, K.; Schmidt, H.; Amberger, E.; Will, G.; Kossobutzki, K. H. *J. Less-Common Met.* **1972**, *29*, 161.

S0897-4756(96)00352-3 CCC: $14.00

morphology and the relationship between the microstructure and properties from the preparative details is required.

We describe herein the synthesis, the surface modification, subsequent deposition and phase evolution of Ti−B−N thin films on glass surfaces and optical fibers. Morphological characterization of the films present challenges associated with the small grain size and light element variations that are met with the surface analytical techniques of polycrystalline X-ray diffraction (XRD), Rutherford backscattering spectroscopy (RBS), Auger electron spectroscopy (AES), scanning electron microscopy (SEM), and atomic force microscopy (AFM). The electrical, mechanical, and physical−chemical behavior of the films in the temperature range 500−700 °C were studied. Experimental details related to processing are reported, and the film characterization and ceramic phase formation are discussed. Finally, the results are summarized with respect to implications of the fabrication of unprecedented dual functional ("two-in-one") optical fibers.

Experimental Section

Synthesis. We have studied the deposition of Ti−B−N on SiO_2 substrates using borazine[19,20] and diammonium hexafluorotitanate(IV) ($[(NH_4)_2TiF_6]$, Aldrich). The solid−gas reaction was carried out in a reactor describing the preparation of blue boron nitride thin films in an earlier publication.[13] SiO_2, Si(100), and Si(111) substrates have been used in the present report. However, the adhesion of the films was poor in the case of Si(100) and Si(111). A nitrogen flow rate of 12 mL min^{-1} was maintained during the deposition. The substrates (dimension 5 × 5 and 10 × 10 mm^2) were degreased first with 2-propanol, rinsed with distilled water and treated with hydrofluoric acid for 1 min. They were rinsed again with distilled water and then treated with dry nitrogen prior to film deposition. $[(NH_4)_2TiF_6]$, with a white color was ground to a homogeneous fine powder with particle size on the order of a micrometer. A sample of 0.15−0.25 g of the powder was taken to cover the substrate. This layer had a uniform thickness on the surface of the substrate of about 2 mm. A platinum crucible containing the substrate and the titanium complex were introduced into a quartz tube of a furnace and treated with N_2 (30 min) at room temperature. Then the temperature is increased to 700 °C for 30 min maintaining a borazine gas stream for a period of 1 h. After the deposition was complete the reactor was cooled to room temperature under a nitrogen flow.

Characterization. *RBS Measurements.* Rutherford backscattering spectroscopy was used to analyze the depth distribution of elements in the films. A comprehensive introduction into the RBS technique has been reported.[21] Details concerning the present setup are described.[22] The RBS experiments were carried out at the Göttingen 500 kV ion implanter IONAS[23] at room temperature with 900 keV α-particles under normal incidence. The backscattered α-particles were detected by means of two Si surface barrier detectors at scattering angles of 165°. The detector resolution of typically 13 keV (fwhm) was the effective limitation of the depth resolution $\Delta X \approx 10$ nm, since the energy spread of the α-beam is less than 0.3 keV[23] (fwhm) and straggling inside the sample is about 2−3 keV.[24] The spectra were analyzed with the computer simulation program RUMP. [25]

AES Measurements. Auger electron spectroscopy data were obtained using a Physical Electronics PHI 595 scanning Auger spectrometer at a base pressure of 10^{-9} mbar. The spectrometer was equipped with a cylindrical mirror electron energy analyzer (CMA) having an integral, coaxially mounted electron gun. Auger electron spectra were recorded with an energy resolution of 0.5%. Surface composition of the deposited Ti−B−N films were analyzed. An AES depth profile was obtained using a 3 keV Ar^+ ion beam (current density 1 μA) over an area of 0.2 × 0.2 mm^2. The sputtering rate for the Ti−B−N films was estimated to be 12 nm min^{-1}.

AFM Analyses. Atomic force microscopy was performed using a Nanoscope III (Digital Instrument, Santa Barbara, CA). Head types E and J; E, X: 28.1 nm V^{-1}, Y: 31.0 nm V^{-1}, Z: 5.60 nm V^{-1}; J, X: 328 nm V^{-1}, Y: 377 nm V^{-1}, Z: 11.6 nm V^{-1}; 256 × 256 points; E_{max}: X, 12 364 nm, Y, 13 640 nm, Z, 2462 nm; J_{max}: X, 144 320 nm, Y, 165 880 nm, Z, 5104 nm; asymmetric Si tips with 17° and 25° vertex angles; cantilever with spring constant 23−92 N m^{-1}; images were taken in constant height mode, plane-fit, and low-pass filter. Measurements made on several films were reproducible. Cross-sections were obtained for each sample in the depth-profile analysis. Measurements were made from the base of each peak to its maximum height. X-ray diffraction spectra were obtained using a Siemens D500 diffractometer and monochromated Cu Kα radiation ($\lambda = 154.18$ pm). Vickers hardness[26,27] of the films was determined using a diamond indenter with a load of 100p. At least 10 indentations were made at the applied load (each indentation for 20 s), and both diagonals were measured using an optical microscope. The electrical resistivity of the films was measured. The bulk resistivity is given by the product of the sheet resistance and the thickness of the film. The sheet resistance was determined using a four-point probe.

Results and Discussion

To optimize the temperature of deposition (600−700 °C) of Ti−B−N films, preliminary deposition experiments were performed. Black films of Ti−B−N were observed to appear initially at 600 °C. The optimal temperature for growing the highest quality films was 700 °C, using a reaction time of 1 h. To understand the mechanism of the reaction between $[(NH_4)_2TiF_6]$ and $B_3N_3H_6$ for the deposition of Ti−B−N films, it was necessary to perform the following control experiments. It is well understood that $[(NH_4)_2TiF_6]$ decomposes at approximately 300 °C to afford NH_4F and TiF_4[28] and borazine at approximately 500 °C to afford BN and H_2.[29] We have studied the reaction of TiF_4 with $B_3N_3H_6$ at 700 °C and found evidence of Ti−B−N formation; however, the adhesion to SiO_2 substrates is poor. The reaction of NH_4F with $B_3N_3H_6$ at 700 °C affords a white boron nitride with good adhesion to SiO_2 substrates. We infer from these observations that the decomposition products of $[(NH_4)_2TiF_6]$ are essential for the deposition of Ti−B−N films with strong surface adhesion. Furthermore, the titanium compound presumably serves two functions: to generate the HF ($NH_4F \rightarrow NH_3 + HF$) necessary for surface modification of the SiO_2 substrates and the titanium for the deposition of Ti−B−N. The resulting Ti−B−N films processed in this manner exhibit high hardness and crystallinity of the surface. In addition, we were successful in the coating of communications grade optical fibers (OF) with the Ti−B−N ceramic under the optimized reaction conditions.

(19) Schaeffer, R.; Steindler, M.; Hohnstedt, L.; Smith Jr., H. S.; Eddy, L. B.; Schlesinger, H. I. *J. Am. Chem. Soc.* **1954**, *76*, 3303.
(20) Wideman, T.; Sneddon, L. G. *Inorg. Chem.* **1995**, *34*, 1002.
(21) Chu, W. K.; Meyer, J. W.; Nicolet, M. A. *Backscattering Spectroscopy*; Academic Press: New York, 1978.
(22) Bolse, W. *Mater. Sci. Eng.* **1994**, *R12*, 53.
(23) Uhrmacher, M.; Pampus, K.; Bergmeister, F. J.; Purschke, D.; Lieb, K. P. *Nucl. Instrum. Methods* **1985**, *B9*, 234.
(24) Chu, W. *Phys. Rev.* **1976**, *A13*, 2057.
(25) Doolittle, L. R. *Nucl. Instrum. Methods* **1986**, *B15*, 227.
(26) Kussmaul, K. *Lexikon Werkstofftechnik*; Gräfen, H., Ed.; 409 VDI: Düsseldorf, 1991.
(27) Münz, W. D. *J. Vac. Sci. Technol.* **1986**, *A6*, 2717.
(28) Ginsberg, H.; Holder, G. *Z. Anorg. Allg. Chem.* **1931**, *201*, 198.
(29) Fazen, P. J.; Jeffrey, S. B.; Lynch, A. T.; Remsen, E. E.; Sneddon, L. G. *Chem. Mater.* **1990**, *2*, 96.

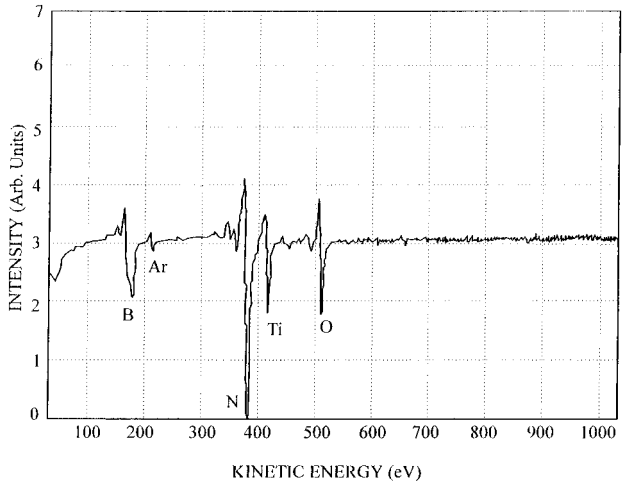

Figure 1. First derivative Auger electron survey spectra showing the principal Auger transition peaks for Ti−B−N film after 32 min sputtering.

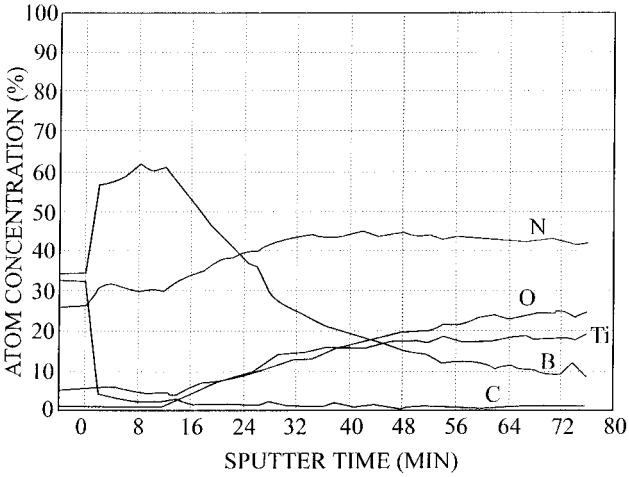

Figure 2. Auger depth profile of Ti−B−N film deposited on SiO_2 substrate at 700 °C for 60 min.

The results of AES analyses of a Ti−B−N film after 32 min sputtering is shown in Figure 1. As can be seen, the film consists of titanium, boron, and nitrogen. The presence of oxygen in the film is probably due to the interfacial diffusion caused by the decomposition products of $[(NH_4)_2TiF_6]$ at the surface of the substrates. To study the stoichiometry of the film, AES depth profile is obtained and shown in Figure 2 for a film prepared at 700 °C for 1 h processing. One can see that, during the first 16 min of sputtering (≈200 nm in depth), no titanium is found in the layer; and for this thickness the film can be considered as a layer having a "boron-rich boronitride" composition with a stoichiometry of [B]:[N] close to 2. As the sputtering time increases (>16 min), we observe simultaneously a progressive increasing of the titanium concentration with the oxygen concentration. Figure 3 shows the variation of the concentration ratios of [Ti]/[B] and [B]/[N] as functions of the sputtering time. As expected, the [Ti]/[B] ratio increases linearly with the sputtering time whereas the [B]/[N] ratio decreases from an initial value of 2 to a constant value of about 0.23. This finding is corroborated by our RBS measurements performed on films prepared at 700 °C for 30, 60, and 90 min processing time. In Figure 4 the RBS spectra are shown in comparison to a TiO_x film ($x \approx 2$). In all cases the resulting film is subdivided into a thin layer near the surface, which does not contain significant amounts of

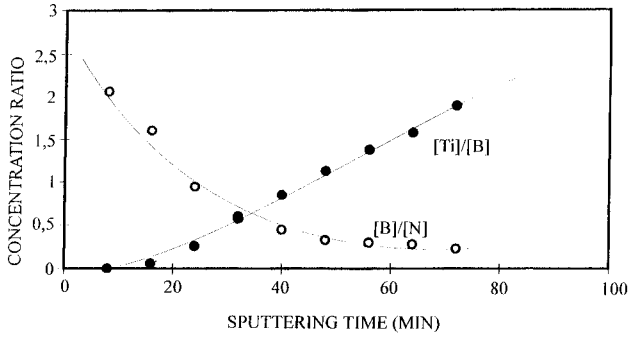

Figure 3. Concentration ratios [B]:[N] and [Ti]:[B] as measured by AES as a function of sputtering time.

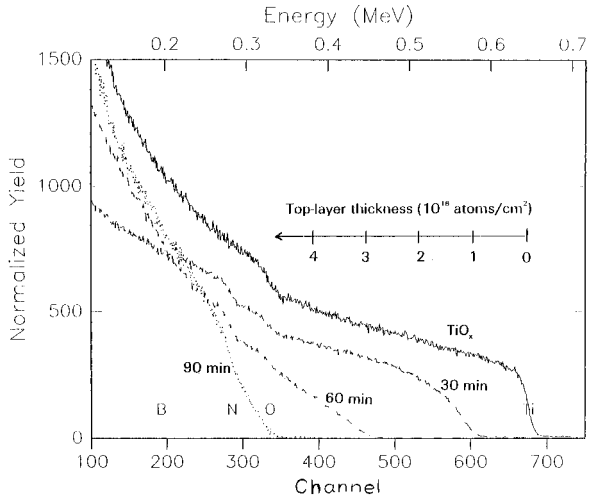

Figure 4. RBS spectra of coatings prepared at 700 °C and the indicated processing times in comparison with the RBS spectrum of TiO_x ($x \approx 2$). The shift of the Ti edge is a measure of the thickness of the Ti-free layer.

Ti, and a subsequent Ti-rich layer extending to the interface. By comparison of the Ti RBS yields of the film processed for 30 min and the oxide layer, the Ti content in the Ti rich part of the film can be estimated to be about 20 at. %, which is in good agreement with the AES profile shown in Figure 2. The area density $d = t\rho$ of the Ti-free layers (which is the product of its geometrical thickness t and its density ρ) which can be estimated from the shift of the Ti edge in the RBS spectra with respect to the TiO_x film increases from 1000 atoms/cm^2 for 30 min processing to about 3000 atoms/cm^2 for 60 min and roughly 4750 atoms/cm^2 for 90 min processing time. If we take the atomic density of BN, $\rho = 1.08\ 10^{23}$ atoms/cm^3, as an estimate of the unknown density of the film, the thickness $t = d/\rho \approx 280$ nm of the B_xN ($x \approx 2$) top layer produced at 60 min processing time compares well with AES results shown in Figure 2. From the AES and RBS analyses, one can say that there are simultaneously two features occurring during the decomposition process of $[(NH_4)_2TiF_6]$: deposition of titanium from TiF_4 as a first layer on the substrate and, at the same time the resulting NH_4F is involved in the reaction on the surface of SiO_2 substrate with surface modification and diffusion of the oxygen through the layer. This diffusion of oxygen along with the etching of the surface by HF, likely supports the strong adhesion of the film on the substrates. Gissler et al. have observed that good adhesion on substrates such as Si(111) or Corning glass was obtained if titanium was deposited as the first layer.[10] It must be noted that for their coatings, they have used a deposition of a multi-

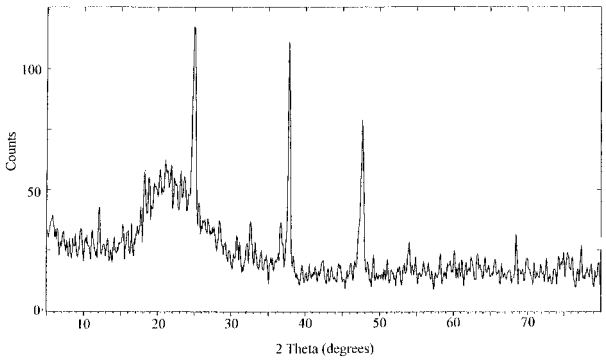

Figure 5. X-ray diffraction pattern of Ti−B−N film deposited on SiO_2 substrate at 700 °C.

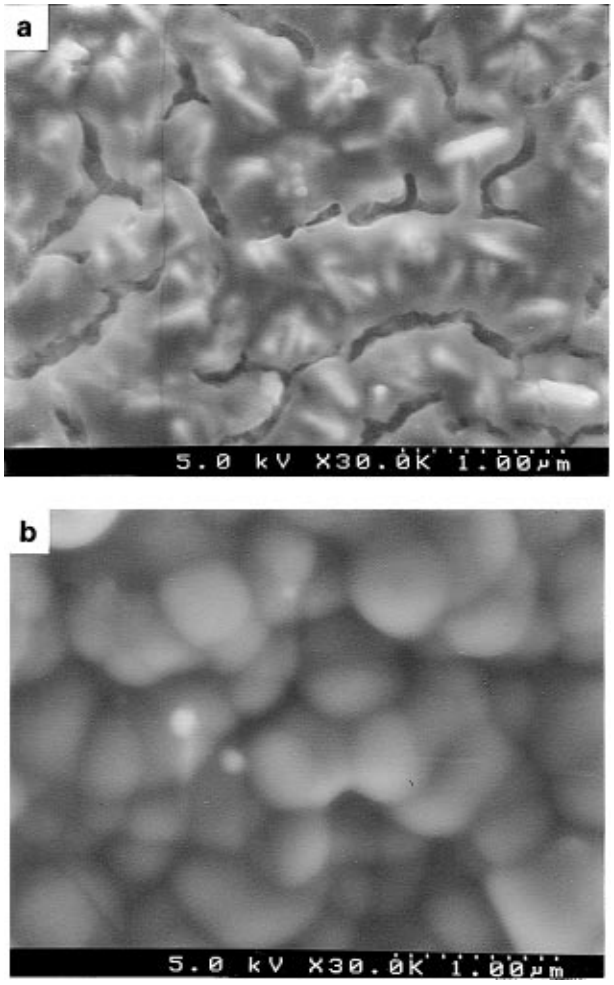

Figure 6. SEM micrographs of Ti−B−N film (a) deposited on SiO_2 substrate and (b) coated on an optical fiber.

layer of the sequence Ti−BN by reactive or nonreactive sputtering from titanium and hexagonal BN target, respectively, and finally a thermal treatment for inducing a diffusion process between the titanium and BN. Moreover, the deposition of titanium as the first layer is common practice to improve the adhesion of TiN coatings.[30] During our study, the surface modification of the substrates and the deposition of Ti−B−N films occurred in one step. This new technique has the advantage that reproducible films with good adhesion to SiO_2 substrates are obtained.

XRD of the black, Ti−B−N films is shown in Figure 5. Three characteristic reflections with relatively high intensities were observed from 5.00 to 80.0° (2θ). These reflections showed no matches with TiN/TiB_2, TiN, TiB_2, BN, $B_{25}N$, B_4C, and rhombohedral B in a JCPDS search.[31] SEM analyses were performed to examine the surface morphology of the Ti−B−N films. Figure 6 shows the SEM images of Ti−B−N as (a) a film on SiO_2

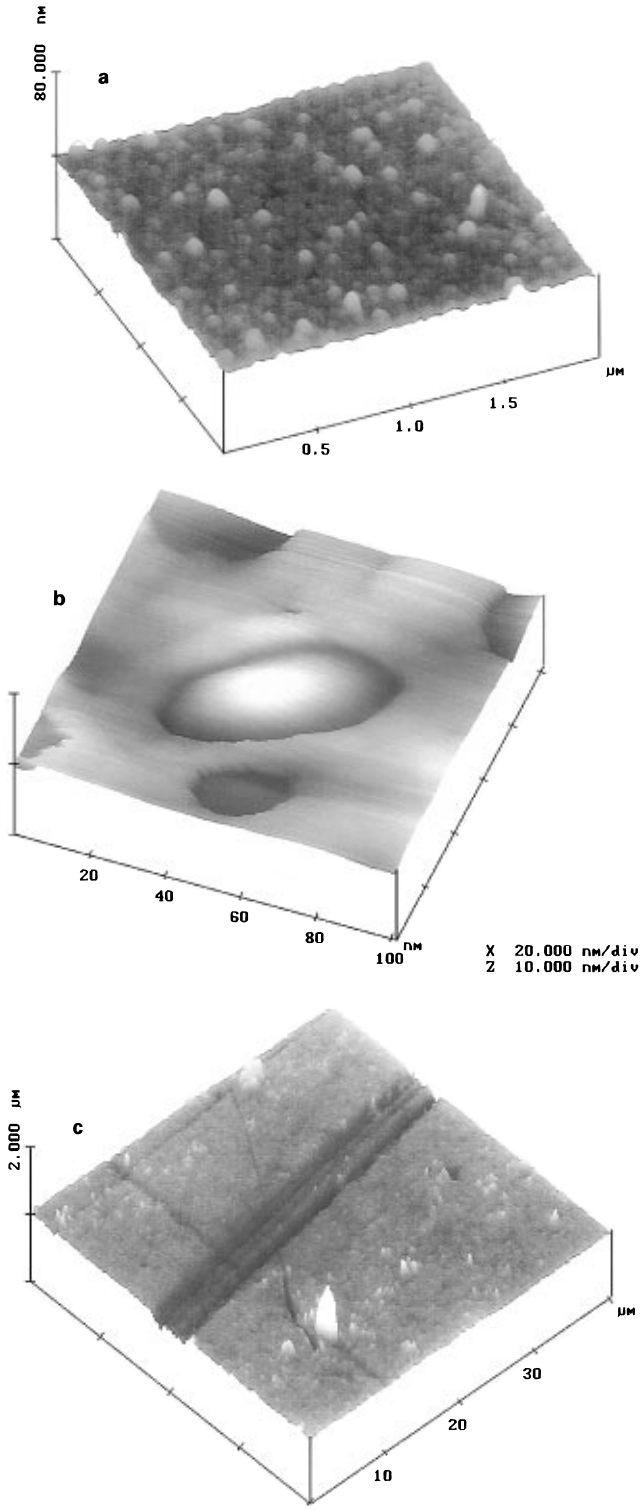

Figure 7. AFM images (in repulsive mode) of the surface of Ti−B−N film deposited on SiO_2 substrate at 700 °C. (a) X: 500 nm/div, Z: 40 nm/div. (b) X: 20 nm/div, Z: 10 nm/div. (c) mechanically deformed film using a quartz cutting tool, X: 10 000 nm/div, Z: 2000 nm/div.

(30) Haefer, R. A.; Ilschner, B. *Oberflächen und Dünnschicht Technologie*; Teil I, Springer: Berlin, 1987.

(31) American Society for Test Materials (ASTM); Berry, L., *et al.*; *Inorganic Index to the Powder Diffraction File*; Joint Committee on Powder Diffraction Standard, Easton, 1971 File No. 38-1420, 35-0741, 35-1365, 25-0098, 35-0798, 31-0207.

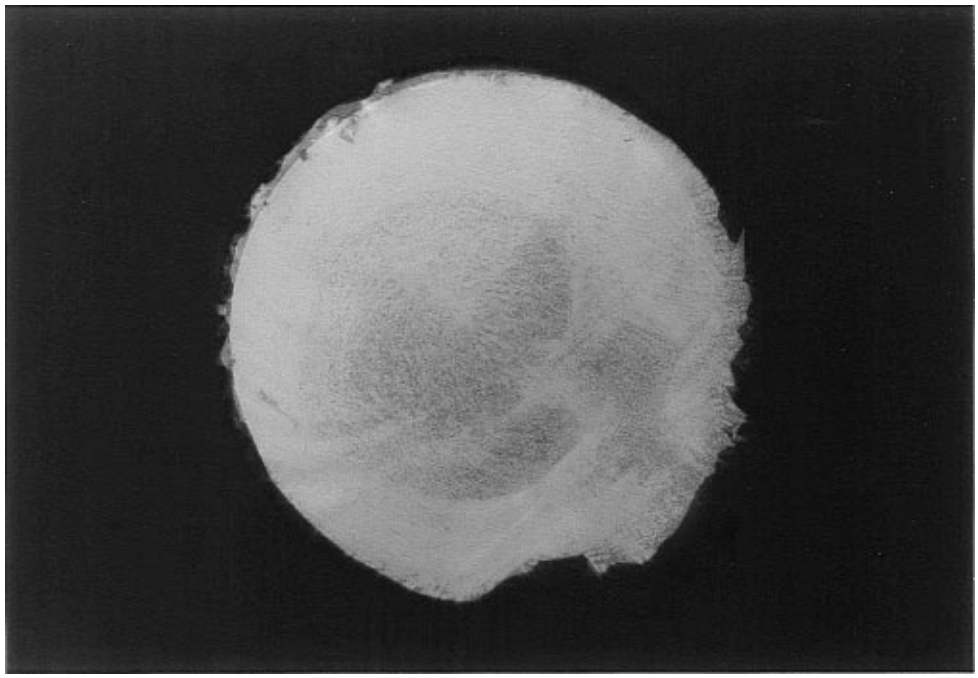

Figure 8. Photograph showing transmission of laser radiation (632.8 nm) through a Ti−B−N coated optical fiber.

and (b) a film on an optical fiber (Sumitomo). Definite grain boundaries are apparent in the film (a), as the presence of large connected regions, separated by channels, and voids are detected. The width of the channels ranges from 10 to 100 nm. Early stages of crystal growth are visible inside the channels and the dominant feature of growth of the film is of the columnar type. In the case of the Ti−B−N film deposited on the optical fiber, homogeneous grain sizes ranging from 200 to 700 nm are observed, indicating a uniform coating. To examine the surface topography in greater detail, AFM was employed and the resulting images (a−c) are summarized in Figure 7. There is good agreement in the grain sizes observed by AFM and SEM (Figure 7a). The columnar growth of the Ti−B−N material can be easily seen from inspection of Figure 7b. The asymmetric Si tip of the AFM follows more closely the surface topography of the film and the columnar growth is examined in more detail. Roughness measurements performed over the entire image and on the top of the column and around the base, using equal areas indicate that the crystal growth occurs on surface specific sites of the substrates (i.e., between columns, there is no appreciable film growth). The surface of the film appears hard and can be mechanically deformed with a quartz glass cutting tool (Figure 7c). The thickness of the Ti−B−N film (Figure 7) is 492 nm from AFM measurements. In general, films deposited on SiO_2 substrates exhibited thicknesses ranging from 0.3 to 1 μm.

Selected mechanical properties of the Ti−B−N material were studied, namely, Vickers hardness and electrical resistivity. Hardness values of Ti−B−N material ranged from 18.07 to 22.35 GPa (1 kp/mm^2 = 9.804 MPa). For comparison, a TiN sample was found to have a HV of 14.26 GPa. The electrical resistivity of the film ranged from 2360 to 5900 $\mu\Omega$ cm. For example, the film of thickness 492 nm (AFM) exhibited a resistivity of 5800 $\mu\Omega$ cm. For comparison, resistivities of TiN films prepared by CVD methods at low temperatures ranged from 200 to 6000 $\mu\Omega$ cm.[32] Furthermore, the measured resistivities were found to be sensitive to oxygen contamination. Moreover it was reported that the bulk resistivity of TiN depends on the ratio of nitrogen to titanium. Titanium and TiN exhibits the lowest resistivities (55 $\mu\Omega$ cm) while TiN_x with $0 < x < 1$ or $x > 1$ tends to show higher resistivities (200−250 $\mu\Omega$ cm).[33] It is obvious that the films of Ti−B−N are within semiconductor/conductor range.

Conclusion

Using solid−gas reaction techniques, we can report the consistent, reproducible processing of Ti−B−N films on a variety of glass substrates using borazine and a diammonium hexafluorotitanate. To our knowledge, this is the first example of a solid−gas reaction and a CVD process.[34] Further, we have realized the first example of optical fibers with "two-in-one" properties, i.e., fibers that carry optical core signals and electrical signal on the external surface. During processing of the Ti−B−N coatings, the optical properties (e.g., transmission of red light) are not diminished. This is shown in Figure 8. Presently we are improving and extending our methodology of CVD process to technologically relevant materials and systems.

Acknowledgment. We thank the Deutsche Forschungsgemeinschaft and the National Science Foundation for support of this work. We also thank H. Guo, K. Keller, Dr. L. Martinez, Dr. A. Perrin, Dr. C. Perrin, J. Rahman, and Dr. J. Stencel for providing measurements. Finally, we are thankful to the Central Electron Microscopy Research Foundation (U. Iowa) and the Institut für Oberflächentechnik und Plasmatechnische Werkstoffentwicklung (U. Braunschweig) for providing facilities and instruments.

CM960352Y

(32) Krutz, S. R.; Gordon, R. G. *Thin Solid Films* **1986**, *140*, 277.
(33) Wittmer, M.; Studer, B.; Melchior, H. *J. Appl. Phys.* **1981**, *52*, 5722.
(34) Hampden-Smith, M. J.; Kodas, T. T. *Chem. Vap. Depos.* **1995**, *1*, 8.